Conformation and electronic structure of DNA in carbon nanotubes: a molecular dynamics and first-principles study

Zha Goujun ✉, *Zhang Fayun* ✉

Xinyu University, Xinyu, People's Republic of China
✉ *E-mail: 393027113@qq.com, zhaguojun_8@163.com*

Published in Micro & Nano Letters; Received on 2nd February 2017; Revised on 15th March 2017; Accepted on 15th March 2017

The conformation and electronic structure of DNA in single-walled carbon nanotubes (SWCNT) were studied by combining molecular dynamics and first-principles methods. It was found that the π orbital of the SWCNT inner wall induces a conformational change in single stranded DNA (ssDNA) and promotes the adsorption of general-sequence oligonucleotides on the inner walls of the SWCNTs due to π–π stacking interactions. Moreover, they found that the adsorbed oligonucleotides form a helix because of electrostatic and torsional interactions within the sugar–phosphate backbone.

1. Introduction: Single-walled carbon nanotubes (SWCNT) have found great utility in electronics detection, optics, mechanics, and heat transport [1, 2], especially in the field of biological and chemical sensing [3, 4]. In addition, their interactions with biological molecules have received widespread attention in recent years [5, 6]. Compared with biological systems, SWCNT are newer and more complex systems. Recently, molecular dynamic (MD) simulations demonstrate that SWCNT can be utilised as molecular channels for transferring water in DNA and RNA [7–9]. This is important because nanotube flow channels used for confining and transporting molecules are ubiquitous in biology and chemistry.

DNA is a complex long-chain polymer comprising deoxyribonucleic acid, usually generated through complementary base pairing of nucleotide bases. DNA is held together by hydrogen bonding of the double helix, and base pairs are matching bases linked by hydrogen bonds, hydrogen bonds can be broken and rejoined with relative ease because they are not covalent. SWCNT have excellent physical properties because of complete covalent sp^2 hybridisation, and they are characteristic of a graphene sheet without defects. Since the sp^2 carbon of SWCNT easily forms a non-covalent π–π bond with an aromatic ring, the structural changes of the aromatic can occur. Many studies [10–21] demonstrate that π stacking of the aromatic bases of DNA and the graphene-like surface of carbon nanotubes (CNT) prevent DNA–CNT interactions. Johnson and colleagues [17, 18] performed classical all-atom MDs simulations to explore the self-assembly mechanisms, structure, and energetic properties of DNA–CNT interactions. Studies have shown that CNT induce natural conformational changes in a single-stranded DNA (ssDNA), and DNA adsorption on CNT surfaces through π–π stacking of the base pairs.

The transfer of DNA or RNA along a CNT channel has been reported both experimentally and through theoretical calculations [5, 8]. Zhou *et al.* [5] reported the translocation of multi-walled CNTs in breast cancer cells and demonstrated that the tube has the ability to target the cytoplasm when there is no cell membrane damage. Gao *et al.* [8] reported on MDs simulations that show a DNA molecule could be spontaneously inserted into a carbon nanotube in water solution. Liu *et al.* [22] reported stable polymer-SWCNT complex can be formed via the multivalent π–π stacking interaction of the lateral pyrene functional groups and the polyfluorene backbone with the outer surface of carbon nanotubes, and the lateral alkyl chains can impart good solubility to the complex.

Recently, Lindsay and Nuckolls reported that the electrophoretic transport of small ssDNA oligomers through CNT is marked by large transient enhancements in ion current. The authors suggest that one of the important reasons for the increase in ion current is a change in DNA conformation during ssDNA translocation though the CNT. Hence, understanding how CNT affect the structure of DNA is highly valuable. To determine the general characteristics of DNA in CNT, we simulated a 12-base random sequence (rand14) adsorbed on the inner wall of the CNT in a water solution. The force field and *ab initio* quantum mechanical methods employed in this paper have provided detailed information regarding the geometry, energetics, and electronic features of single DNA nucleosides adsorbed onto single-wall CNT. We found that the ssDNA undergoes important conformational changes, which leads to the natural adsorption of DNA on the inner wall of the CNT and interactions between the inner wall of the SWCNT and DNA base through π–π stacking. Moreover, we discovered that hydrogen bonds form between adjacent DNA bases during DNA adsorption on the inner wall of the CNT.

2. Experimental: We performed MDs simulations under constant pressure (1 atm) and constant temperature (300 K) with the GROMACS MD package using a 1 fs time step. We used the AMBER99 force field [23] to model ssDNA. On the basis of previous studies [9, 24], we modelled the SWCNT atoms as uncharged Lennard–Jones particles using sp^2 carbon parameters from the AMBER99 force field. Electrostatic interactions were determined using the particle mesh Ewald method. In the AMBER99 force field, stacking interactions among aromatic species are parametrised within the van der Waals parameters of each atom type. Specific electrostatic interactions among δ electrons are averaged. We performed all simulations with an explicit solvent using the TIP3P water model [25].

Classical MDs simulations are carried out to determine the binding of ssDNA on the inner wall of an SWCNT. The sizes of the simulation box were initially set to $5 \times 5 \times 8$ nm. The primary simulation system consisted of the SWCNT fastened along the z-axis at the centre of the box. We chose a (18, 18) zigzag SWNT containing 2400 carbon atoms. The simulation was initially performed on a random oligonucleotide containing 12 bases in the centre of SWCNT. The ssDNA was initialised in a helical-stacked conformation, which is a reasonable structure for short

doi: 10.1049/mnl.2017.0030

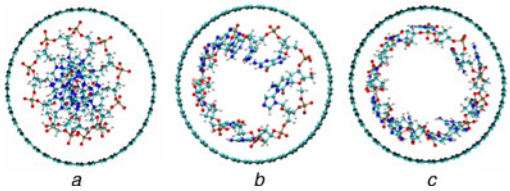

Fig. 1 *Simulation of ssDNA adsorption on the inner wall of carbon at different times*
a Initial configuration
b Configuration after 2 ns
c Configuration at 7 ns

oligonucleotides in aqueous solutions. The time step was 2 fs. The time step of 2 fs, reference temperature of 300 K, and isotropic coupling pressure was chosen from the Berendsen scheme with a coupling constant of 1.0 ps. The reference pressure in all directions is 1 bar. The goal of using the steepest descent method was to minimise system energy. At an equilibrium temperature of 300 K and friction constant of 0.5 ns, a long run was performed with a leapfrog stochastic dynamics integrator.

The first-principles calculations are based on pseudopotentials derived from the density functional theory as implemented in SIESTA [26, 27]. The Ceperley–Alder version of the local density approximation (LDA) was used for electron exchange and correlation [28], and the optimised Troullier–Martins [29] pseudopotentials were used for the atomic cores in this calculation. A linear combination of numerical atomic orbitals with double-ζ polarisations is used in the basis set to describe the valence electrons [30]. Real space integration was performed on a regular grid corresponding to a plane-wave cutoff around 200 Ry, for which the structural relaxations and electronic energies are fully converged. Previous studies [31] have indicated that LDA attained a good result for CNT studies.

3. Results and discussion: To obtain microscopic images of ssDNA on the inner wall of an SWCNT, a simulation was carried on a random oligonucleotide containing 12 based, initially in the centre of an (18,18) SWCNT (Fig. 1*a*). ssDNA exhibits a spiral stacking structure, which is reasonable for short oligonucleotides in aqueous solution. Within the first 2 ns, several ssDNA segments make contact with the inner wall of the CNT. These fragments lead to a conformational change, which is rotated by ∼30° relative to the nucleotide sugar phosphate backbone, thus separating from its neighbours. This enables the accumulation of the individual base pairs on the inner surface of DNA with a weak surface of the CNT. We found that these bases form tightly against the inner wall of the CNT and strongly depend on the inner wall of the CNT (Fig. 2b). At 7 ns, most of the nucleobases are adsorbed on the inner wall of the SWNCT (Fig. 1*c*).

The rotating motions of the bases along the backbone of DNA were analysed using a pseudo-dihedral angle defined by the angle of the two planes shown in Fig. 3*A*: the base plane, A, and the sugar plane, B. Fig. 3*B* shows the dihedral angle as a function of

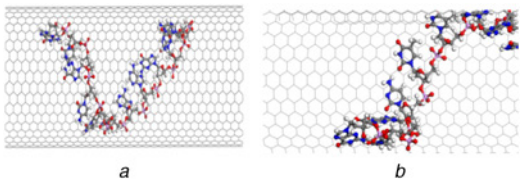

Fig. 2 *Side view of ssDNA adsorption on the inner wall of carbon nanotube at 20 ns*
a main view
b side view

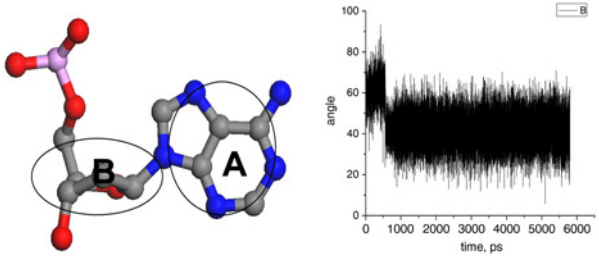

Fig. 3 *Angel between base and sugar plan as time*
A Pseudo-dihedral angle
B Dihedral angel

time. From Fig. 3, the initial dihedral angle between A and B is ∼70°. At 0.5 ns, the dihedral angle is slightly enlarged because of the elongation of the DNA chain during the simulation. At the 0.7 ns, the dihedral angle decreases from 75° to 40°. The decreasing dihedral angle leads to facile interactions between the base and the inner wall of the SWCNT. As shown in Fig. 1*b*, nearly the entire ssDNA backbone is closer to the inner wall of the SWCNT, which allows the extra base to interact with the inner wall. In the following 7 ns, many of the remaining non-bound nucleobases adsorb to the inner wall of the SWCNT. In addition, ssDNA spontaneously wraps around a left-handed helix and adsorbs on the inner wall of the SWCNT. Fig. 4 shows the average distance between the base and the inner wall of the CNT during the simulation. In fact, in initial helical conformation, the distance between the base and inner wall of the CNT is ∼16 Å. Subsequently, at 0.7 ns, the distance significantly decreases from 16 to 6 Å, which indicates that there are parts of the bases that interact with the inner wall of the CNT through π–π stacking. At 2.0 ns, the distance is spontaneously reduced to 3.6 Å. This indicates that before 3 ns, most of the DNA bases nearly interact with the inner wall of the CNT via π–π stacking. Moreover, the motions of the base clearly correlate with the π–π stacking distance between the DNA bases and CNT, which also results in the elongation of the ssDNA backbone. The structural change of DNA in CNT is driven by strong van der Waals attraction between the DNA base and the inner wall of the CNT due to π–π stacking. Furthermore, the hydrogen bond between adjacent nucleobases significantly contributes to the total bond energy (Fig. 2*b*). Since the driving forces for helix formation and ssDNA adsorption are independent of the specific base sequence, the general ssDNA sequence is expected to package SWCNT in a similar way is generally observed here.

Since the methods discussed currently rely on the force-field-derived vdW interactions and electron charge polarisation explicitly leads to nucleoside–CNT interactions, density functional theory (DFT)/LDA methods used for understanding quantum interactions must be explored. To understand the mechanisms behind the interactions on an electronic level, the force-field calculation using the

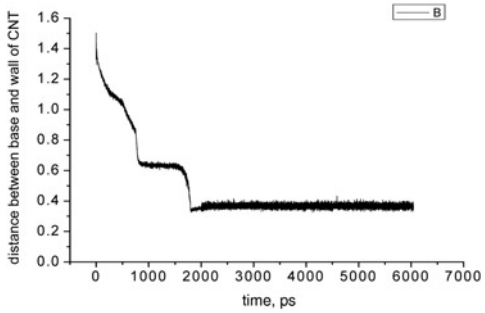

Fig. 4 *Distance between base and wall of CNT as time*

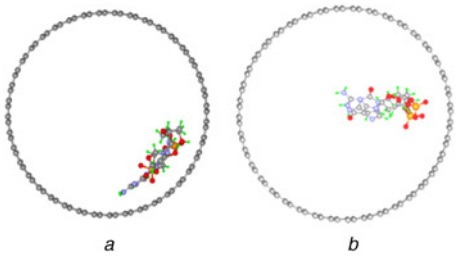

Fig. 5 *Equilibrium geometries of DNA in CNT*
a forming structure A
b forming structure B

DFT/LDA method was further optimised. In this study, the adsorbed molecules include a phosphate salt bridge to connect two adenine nucleoside molecules, and the termination of the sugar rings with a hydrogen bond was stopped to produce an electronic environment for nucleic acid bases, it is similar to a more intimate situation, not for a single-isolated base. DNA adsorption in the (18,18) CNT was studied using two models: ssDNA backbone molecular axes (A) parallel and (B) perpendicular to the tube axis (Fig. 5). The local structure (A), i.e. covalent bond lengths and bond angles, exhibits minor changes compared with the MD results. The distance between the base and inner wall of the CNT in Structure A is ~3.2 Å, which is slightly shorter than that in the MD study. Moreover, the distance between base and inner wall of the CNT in Structure B is 3.97 Å, which is larger than in Structure A. Slight curvature around the nanotube is shown to maximise the bulk interactions of the base unit, which is similar to the results from MD simulations. According to previous calculations [20], we found that sugar residues were more flexible. Evidence shows that the interactions between sugar residues and CNT are non-covalent.

The adsorption energy of the DNA–CNT system was calculated using the following equation:

$$\mathrm{EB} = E(\mathrm{DNA/SWNT}) - E(\mathrm{DNA}) - E(\mathrm{SWNT}),$$

where E(SWNT) is the total energy for the isolated pristine tube, E(DNA) is total energy of isolated DNA molecule and E(DNA/SWNT) is the total energy of the DNA adsorbed on the SWNT.

The calculated interaction energy is 1.72 and 0.98 eV for Structures A and B, respectively. The interaction energy of Structure A is low in comparison to the two absorption energies of graphite according to the thermal absorption spectrum and is lower than that of DNA adsorbed on a CNT. Moreover, in our dual system, the DNA is made up of two adenine molecules, which have four aromatic rings. Therefore, in this combined system, the absorption energy may largely result from the contribution of the four aromatic groups.

The density of states (DOS) of the isolated CNT, the isolated DNA and their combination, DNA@CNT, are displayed in Fig. 6. The Fermi energy level (Ef) of CNT was −2.18 eV, while

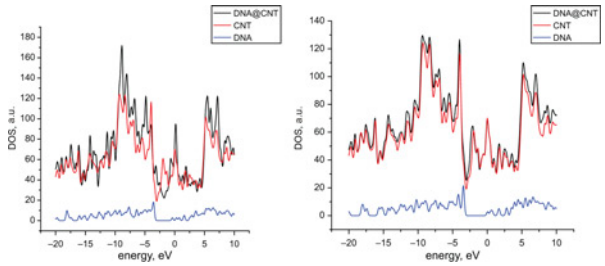

Fig. 6 *DOS for structure A and B*

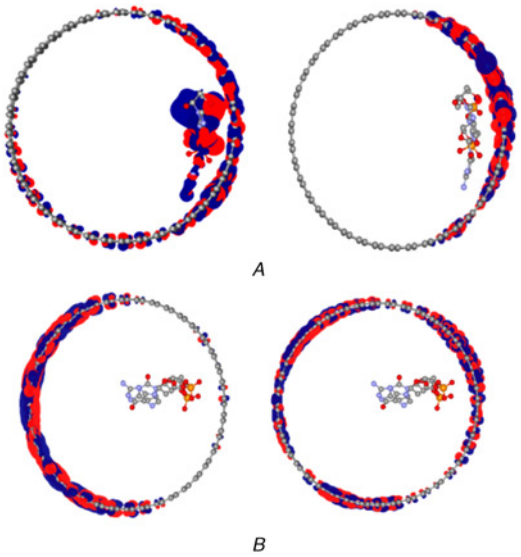

Fig. 7 *Isosurface of the wave functions of the HOMO (left panel) and LUMO (right panel) for A and B*

for the DNA@CNT, the Ef was −2.38 and −2.26 eV for Structures A and B, respectively, which implies that the non-valent interaction between DNA and the CNT in Structure A has a greater effect on the electronic structure of DNA@CNT than in Structure B. The DOS calculations demonstrate that the nucleobase group contributed important components at the Fermi energy band for Structure A. However, there are no such components for Structure B. The highest occupied molecular orbital(HOMO) and lowest unoccupied molecular orbital(LUMO) of the CNT, DNA and DNA@CNT are given in Fig. 7. Fig. 7 also shows that there are large differences between the electronic structures of A and B. All of these results suggest that the conformational change of DNA in CNTs greatly affects the electronic structure and DOS of CNTs. Lindsay and Nuckolls reported electrophoretic transport of small ssDNA oligomers in CNTs is marked by large transient increases in ion current. Moreover, the conformational change of DNA during transport through the CNT leads to instantaneous maldistribution in electronic density, resulting in a strong ion current. Fig. 8 shows the isodensity surface of the charge density for Structures A and B. The isodensity surface of the charge density for Structure A indicates that the interaction mainly involves the π orbitals in the DNA base and the CNT. However, the polarisation of π orbitals is clearer in Structure A than in Structure B.

In Structure A, the HOMO contribution is largely from DNA. In contrast, for Structure B, both the HOMO and LUMO are mainly derived from the CNT, with no contribution from DNA. This demonstrates that the interaction between CNT and DNA in Structure A is stronger than that in Structure B, where the carbon nanotubes act as the donor and the aromatic molecules act as the acceptor. Additionally, the strong interactions between DNA and the CNT result in DNA structural changes. Moreover, the calculated charge transfer between the CNT and nucleobase indicates that

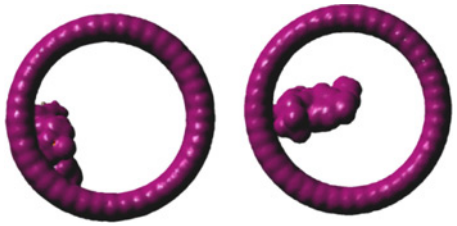

Fig. 8 *Isodensity surface of the charge density difference at levels of 0.0004 e/A3 for A and B*

doi: 10.1049/mnl.2017.0030

there is greater charge transfer from CNT to DNA in Structure A than in Structure B. As demonstrated in Fig. 5, this indicates that there are strong π–π interactions between the CNT and DNA base because of π–π stacking strong orbital hybridisation between CNT and DNA.

4. Conclusion: In conclusion, the conformation and electronic structure of DNA in SWCNTs were studied by using a combination of MDs and first-principles methods. We found that the π orbital of the SWCNT's inner wall induces a conformational change in ssDNA, leading to general-sequence oligonucleotide adsorption through π–π stacking interactions. Simultaneously, interactions between the adsorbed oligonucleotide helix formation and the torsion of the sugar phosphate backbone occur, which leads to a coating of ssDNA on the CNT wall. First-principles calculations indicate that the presence of a strong non-covalent π–π stacking interaction between the nucleobase and the inner wall of the CNT produces the most stable structure. The adsorption energies were 1.72 and 0.98 eV for Structures A and B, respectively.

5. Acknowledgements: We gratefully acknowledged the support of the Natural Science Foundation of China (grant no. 51664047) and the Foundations from the Department of Education in Jiangxi Province (grant no. GJJ161187).

6 References

[1] Star A., Gabriel P., Bradley K., *ET AL.*: 'Electronic detection of specific protein binding using nanotube FET devices', *Nano Lett.*, 2003, **3**, (4), pp. 459–463
[2] Besteman K., Lee J.–O., Wiertz F.G.M., *ET AL.*: 'Enzyme-coated carbon nanotubes as single-molecule biosensors', *Nano Lett.*, 2010, **6**, (1), pp. 27–30
[3] Chen R.J., Zhang Y.G., Wang D.W., *ET AL.*: 'Noncovalent sidewall functionalization of single-walled carbon nanotubes for protein immobilization', *J. Am. Chem. Soc.*, 2001, **123**, (16), pp. 3838–3839
[4] Kam N.W.C., Jessop T.C., Wender P.A., *ET AL.*: 'Nanotube molecular transporters: internalization of carbon nanotube−protein conjugates into mammalian cells', *J. Am. Chem. Soc.*, 2004, **126**, (22), pp. 6850–6851
[5] Zhou X.J., Moran-Mirabal J.M.H., Craighead G., *ET AL.*: 'Supported lipid bilayer/carbon nanotube hybrids', *Nat. Nanotechnol.*, 2007, **2**, (1), pp. 185–190
[6] Wang H., Ceulemans A.: 'Physisorption of adenine DNA nucleosides on zigzag and armchair single-walled carbon nanotubes: a first-principles study', *Phys. Rev. B*, 2009, **79**, (19), pp. 195419
[7] Lu Q., Moore J.M., Huang G., *ET AL.*: 'RNA polymer translocation with single-walled carbon nanotubes', *Nano Lett.*, 2004, **4**, (12), pp. 2473–2477
[8] Gao H., Kong Y., Cui D., *ET AL.*: 'spontaneous insertion of DNA oligonucleotides into carbon nanotubes', *Nano Lett.*, 2003, **3**, (4), pp. 471–474
[9] Hummer G., Rasaiah J.C., Noworyta J.P.: 'Water conduction through the hydrophobic channel of a carbon nanotube', *Nature*, 2001, **414**, (8), pp. 188–190
[10] Dong L., Witkowski C.M., Craig M.M., *ET AL.*: 'Cytotoxicity effects of different surfactant molecules conjugated to carbon nanotubes on human astrocytoma cells', *Nanoscale Res. Lett.*, 2009, **4**, (2), pp. 1517–1523
[11] Staii C.A., Johnson T.C.: 'DNA-decorated carbon nanotubes for chemical sensing', *Nano Lett.*, 2005, **5**, (11), pp. 1774–1778
[12] Gowtham S., Scheicher R.H., Pandey R., *ET AL.*: 'First-principles study of physisorption of nucleic acid bases on small-diameter carbon nanotubes', *Nanotechnology*, 2008, **19**, (12), p. 125701
[13] Zheng M., Jagota A.M., Strano S.A., *ET AL.*: 'Structure-based carbon nanotube sorting by sequence-dependent DNA assembly', *Science*, 2003, **302**, (5650), pp. 1545–1548
[14] Meng S., Wang W.L., Paul M., *ET AL.*: 'Determination of DNA-base orientation on carbon nanotubes through directional optical absorbance', *Nano Lett.*, 2007, **7**, (8), pp. 2312–2316
[15] Johnson R.R., Johnson A.T.C., Klein M.L.: 'The nature of DNA-base–carbon-nanotube interactions', *Small*, 2009, **6**, (1), pp. 31–34
[16] Johnson R.R., Kohlmeyer A.A., Johnson T.C., *ET AL.*: 'Free energy landscape of a DNA−carbon nanotube hybrid using replica exchange molecular dynamics', *Nano Lett.*, 2009, **9**, (2), pp. 537–541
[17] Johnson R.R., Johnson A.T.C., Klein M.L.: 'Probing the structure of DNA−carbon nanotube hybrids with molecular dynamics', *Nano Lett.*, 2008, **8**, (1), pp. 69–75
[18] Johnson R.R., Kohlmeyer A.A., Johnson T.C., *ET AL.*: 'Computational study of a nano-biosensor: A single-wall carbon nanotube functionalized with the coxsackie-adenovirus receptor', *J. Phys. Chem. B*, 2009, **113**, pp. 11589–11593
[19] Chen X., Kis A., Zettl A., *ET AL.*: 'A cell nanoinjector based on carbon nanotubes', *Proc. Natl. Acad. Sci. USA*, 2007, **104**, (20), pp. 8218–8222
[20] Meng S., Wang W.L., Maragakis P., *ET AL.*: 'DNA nucleoside interaction and identification with carbon nanotubes', *Nano Lett.*, 2007, **7**, (1), pp. 45–50
[21] Liu H., He J., Tang J., *ET AL.*: 'Translocation of single-stranded DNA through single-walled carbon nanotubes', *Science*, 2009, **327**, (5961), pp. 64–67
[22] Liu M., Chen Y., Zhu B., *ET AL.*: 'Synthesis of polyfluorenes bearing lateral pyreneterminated alkyl chains for dispersion of single-walled carbon nanotubes', *Chin. J. Polym. Sci.*, 2012, **30**, (3), pp. 405–414
[23] Lindahl E., Hess B., van der Spoel D., *ET AL.*: 'a package for molecular simulation and trajectory analysis', *J. Mol. Model.*, 2001, **7**, (8), pp. 306–317
[24] Zhao X.C., Johnson J.K.: 'Simulation of adsorption of DNA on carbon nanotubes', *J. Am. Chem. Soc.*, 2007, **129**, (34), pp. 10438–10445
[25] Jorgensen W. L.: 'Quantum and statistical mechanical studies of liquids. 10: transferable intermolecular potential functions for water, alcohols, and ethers. Application to liquid water', *J. Am. Chem. Soc.*, 1981, **103**, (2), pp. 335–340
[26] Ordejon P., Artacho E.J., Soler M.B.: 'Self-consistent order-N density-functional calculations for very large systems', *Phys. Rev.*, 1996, **53**, (16), pp. R10441–R10444
[27] Sanchez-Portal D., Artacho E., Soler J.M.: 'Density-functional method for very large systems with LCAO basis sets', *Int. J. Quantum Chem.*, 1997, **65**, (5), pp. 453–461
[28] Ceperley D.M., Alder B.J.: 'Ground state of the electron gas by a stochastic method', *Phys. Rev. Lett.*, 1980, **45**, (7), pp. 566–569
[29] Troullier N., Martins J.L.: 'Efficient pseudopotentials for plane-wave calculations', *Phys. Rev. B*, 1991, **43**, (11), pp. 8861–8869
[30] Artacho E., Sanchez-Portal D., Ordejon P., *ET AL.*: 'Linear-scaling ab-initio calculations for large and complex systems', *Phys. Status Solidi B*, 1999, **215**, (1), pp. 809–817
[31] Lin C.S., Zhang R.Q., Niehaus T.A., *ET AL.*: 'J. phys. chem. C, geometric and electronic structures of carbon nanotubes adsorbed with flavin adenine dinucleotide: a theoretical study', *J. Phys. Chem. C*, 2007, **111**, (11), pp. 4069–4073